PAPER

Check for updates

Ru(II)-(PTA) and -mPTA complexes with N$_2$-donor ligands bipyridyl and phenanthroline and their antiproliferative activities on human multiple myeloma cell lines†

Aleksandra Wołoszyn,[a] Claudio Pettinari, (ID) *[b] Riccardo Pettinari, (ID) [b] Gretta Veronica Badillo Patzmay,[b] Anna Kwiecień, (ID) [c] Giulio Lupidi,[b] Massimo Nabissi,[b] Giorgio Santoni[b] and Piotr Smoleński (ID) *[a]

A series of novel ruthenium(II) 2,2′-bipyridyl (bpy) and 1,10-phenanthroline (phen) derivatives containing PTA (1,3,5-triaza-7-phosphaadamantane) or mPTA (*N*-methyl-1,3,5-triaza-7-phosphaadamantane cation) have been synthesized and fully characterized. Three types of complexes have been obtained, neutral [Ru(N–N)(PTA)$_2$Cl$_2$] (**1**, N–N = bpy and **4**, N–N = phen), monocationic [Ru(N–N)(PTA)$_3$Cl][Cl] (**2**, N–N = bpy and **5**, N–N = phen) and dicationic [Ru(N–N)(mPTA)Cl$_2$][BF$_4$]$_2$ (**3**, N–N = bpy and **6**, N–N = phen). The solid-state structures of four complexes have been determined by single-crystal X-ray diffraction. The cytotoxicity of the complexes has been evaluated *in vitro* against U266 and RPMI human multiple myeloma cells.

1. Introduction

The development of metal anticancer drugs has traditionally focused on cytotoxic platinum compounds although only three platinum drugs are today approved for clinical use worldwide and three additional compounds are approved in individual nations.[1,2] Independent of the nature of the platinum compound used, all platinum drugs are believed to exert their antitumour activity through the same mechanism of action as described for cisplatin.[3] In the search for antitumor drugs with a different spectrum of activity and less side effects than those of platinum drugs, ruthenium compounds appear to be the most promising ones. Ruthenium complexes display antitumor and antimetastatic activity due to their highly tuneable structures, easily constructable octahedral geometry, redox

[a]Faculty of Chemistry, University of Wrocław, ul. F. Joliot-Curie 14, 50-383 Wrocław, Poland. E-mail: piotr.smolenski@chem.uni.wroc.pl
[b]School of Pharmacy, University of Camerino, via S. Agostino 1, 62032 Camerino MC, Italy. E-mail: claudio.pettinari@unicam.it
[c]Faculty of Pharmacy, Wroclaw Medical University, ul. Borowska 211 A, 50-566 Wrocław, Poland

†Electronic supplementary information (ESI) available: Figures containing absorption spectral traces, emission spectra, fluorescence emission spectra, Ru complexes in regulating cell cycles, complexes inducing cell death; table of molar absorption values; table of binding constants; table of binding constants, Stern–Volmer constant and apparent binding constants; tables of cell cycle phases. CCDC 1524973–1524976 for **1**, **3**, **5** and **6**. For ESI and crystallographic data in CIF or other electronic format see DOI: 10.1039/c7dt02051a

activities, photochemical properties and also low systemic toxicity. Ruthenium(III) anticancer compounds NAMI-A and NKP1339 went into clinical trials[4] and also, half ruthenium(II)-arene compounds, containing a completely different metallodrug scaffold, showed good activity in a variety of cancer cell lines.[5–13] Phenanthrolines and bipyridines have been widely used in the construction of a large variety of metal complexes with great potential in many applications,[14–16] and ruthenium(II) complexes containing pyridyl ligands are finding numerous applications ranging from imaging or structure- and site-specific reversible DNA binding agents to therapeutics.[17] Additionally, ruthenium complexes containing polypyridines could combine good water solubility and new electronic properties by introduction of the air-stable and water-soluble aminophosphine, 1,3,5-triaza-7-phosphaadamantane (PTA) or its derivatives into the coordination sphere.[18]

In recent years, the coordination chemistry of PTA has seen a pronounced development driven by the search for water-soluble transition ruthenium complexes as rather potent antitumor,[19] catalytic[20,21] or luminescent agents.[22,23]

Multiple myeloma (MM) is a malignant disorder characterized by uncontrolled monoclonal plasma cell proliferation and accumulation of malignant plasma cells in patients' bone marrow (BM).[24] The outcome of patients with MM has improved in the past decade, in terms of both progression-free survival and overall survival.[25] However, MM remains an almost incurable disease, and several other treatment options should be available for disease control.[25] Ruthenium

complexes, as a single-agent or in combination, were evidenced as promising anticancer drugs,[26] mainly in cancer cells that showed resistance to the usual chemotherapy, showing low toxicity compared with other anticancer drugs.[27] Since Ru complexes were previously found to be effective in U266 and RPMI MM cells,[28] herein, we evaluated the cytotoxic effects of new Ru complexes in the same MM cell model, which is a model with a cytogenetic abnormality (loss of 17p) that in patients is associated with a poor outcome.[29]

2. Results and discussion

2.1. Synthesis and characterization

Treatment of $[RuCl_2(COD)]_n$ with a stoichiometric amount of bpy or phen, in EtOH solution under reflux conditions, followed by the addition of a stoichiometric amount of PTA or $[mPTA][BF_4]$ (*i.e.*, Ru:N–N:PTA and Ru:N–N:mPTA molar ratios of 1:1:2), leads to $[RuCl_2(N–N)(PTA)_2]$ {N–N = bpy (**1**), phen (**4**)} and $[RuCl_2(N–N)(mPTA)_2][BF_4]_2$ {N–N = bpy (**3**), phen (**6**)} discrete coordination compounds (Scheme 1). The reactions of $[RuCl_2(COD)]_n$ with bpy/phen and PTA in a Ru:N–N:PTA molar ratio (1:1:3) under the same conditions afford $[RuCl(N–N)(PTA)_3]Cl$ {N–N = bpy (**2**), phen (**5**)} complexes. Surprisingly, the use of the more sterically hindered $[mPTA]^+$ instead of the PTA ligand under similar conditions (Ru/N–N/mPTA of 1:1:3) also gives rise to the formation of complexes with the general formula $[RuCl_2(N–N)(mPTA)_2][BF_4]_2$. The novel compounds **1–6** have been isolated as air stable, orange (**1**, **3**), dark-orange (**2**) and dark-red (**4–6**) microcrystalline solids in *ca.* 45–81% yields based on $[RuCl_2(COD)]_n$, and characterized by IR, ^1H and $^{31}P\{^1H\}$ NMR spectroscopy, ESI$^+$-MS, elemental analyses and single-crystal X-ray diffraction (for **1**, **3**, **5** and **6**). A noteworthy feature of **1–6** concerns their hydrosolubility, with the $S_{25\ °C}$ values ranging from 11 to 14 mg mL^{-1}. Water solutions are relatively stable in the range of pH = ±2 in air (see section 4.4). In addition, these compounds are soluble in other polar solvents, such as DMSO, acetonitrile and DMF. They are also soluble in middle polar solvents like CHCl$_3$ or CH$_2$Cl$_2$ whereas they are insoluble in

apolar solvents like Et$_2$O, toluene and CCl$_4$. Their strong hydrophilic properties were confirmed by the determination of the negative log P values, corresponding to the octanol–water partition coefficient for **1–6** (see section 4.5). The solution ^1H NMR spectra of **1** and **4** in the PTA region exhibit two types of methylene protons, the first, P–CH$_2$–N, occurring as a singlet at δ 3.52 and 3.40, and the second, N–CH$_2$–N, displaying an AB spin system centred at δ 4.18 and 4.10, respectively. The ^1H NMR spectra of **2** and **5** exhibit double, overlapped sets of methylene protons in the PTA region as multiplets in the 4.32 and 4.60 ppm range. This is due to the non-equivalent positions of PTA ligands in the coordination sphere, in an integral ratio of 2:1 (see Scheme 1) as reported in other compounds.[18,30–33]

The solution ^1H NMR spectra of **3** and **6** exhibit four types of methylene protons and one type of methyl proton in the mPTA region. Three of them: PCH$_2$N, NCH$_2$N and NCH$_2$N$^+$ (centred at δ 3.49, 3.36; 4.21, 4.13 and 4.80, 4.75 for **3** and **6**, respectively) are the AB or ABX type (X = P), assigned to the N–CH$_{ax}$–X and the N–CH$_{eq}$–X (X = N and P) protons, as reported in other compounds.[34] In the case of PCH$_2$N$^+$ and N$^+$CH$_3$ two singlets at δ 4.19, 4.13 and 2.62, 2.57 for **3** and **6**, respectively, have been observed. In the aromatic region, the ^1H NMR spectra of **1–6** also show the resonances due to phenyl rings of bpy and phen coordinated to Ru(II). However the ^1H NMR spectra of **1**, **3**, **4** and **6** display a set of four resonances due to CH protons in the δ 7.58–9.69 region, whereas **2** and **5** show a double set of signals, each set being due to a non-equivalent aromatic ring of bpy and phen, as a consequence of the asymmetric coordination environment experienced by the nitrogen ligands.[35] Integration of the ^1H NMR spectra of **1**, **3**, **4** and **6** confirmed the 1:2 molar ratio of coordinated N–N:PTA or N–N:mPTA ligands and the 1:3 molar ratio of $[Ru(N–N)(PTA)_3]$ complexes (**2** and **5**). The $^{31}P\{^1H\}$ NMR spectra of **1–6** are typical for coordinated PTA (**1**, **2**, **4** and **5**) and mPTA (**3** and **6**) ligands, which are shifted downfield with respect to the uncoordinated PTA and mPTA ligands, showing the corresponding singlets at δ −53.3, −31.4, −53.7 and −31.8, for **1**, **3**, **4** and **6**, respectively. This shows that the **1**, **3**, **4** and **6** are octahedral complexes, and the PTA ligands occupy the axial positions. The ^{31}P NMR spectra of **2** and **5** consist of two signals: a triplet at δ −38.2 and −38.3 and a doublet at δ −57.4 and −58.3 with $^2J_{PP}$ = 34.8 and 34.4 Hz, respectively. This further suggests that the cations in **2** and **5** exhibit a meridional coordination. The IR spectra of **1–6** exhibit absorptions due to the typical vibrations of polypyridine and PTA ligands.[18,30,36] Additionally, the IR spectra of compounds containing BF$_4^-$ anions also show the characteristic strong and broad absorptions centered at 1065 and 1077 cm^{-1} for **3** and **6**, respectively.[36] The formulations of **1–6** are further confirmed by the ESI$^+$-MS spectra of their MeOH solutions, showing peaks due to $[RuCl(N–N)(PTA)]^+$ and/or $[RuCl(N–N)(PTA)_2]^+$, $[RuCl_2(N–N)(mPTA)]^+$, $[RuCl(BF_4)_2(bpy)(mPTA)_2]^+$, respectively, with the expected isotopic patterns. Besides, peaks due to the $[RuCl_2(N–N)(PTA)Na]^+$ and/or $[Ru(N–N)(PTA)_2Na]^+$ ionic fragments are seen in the spectra of complexes **1** and **4**, respectively.
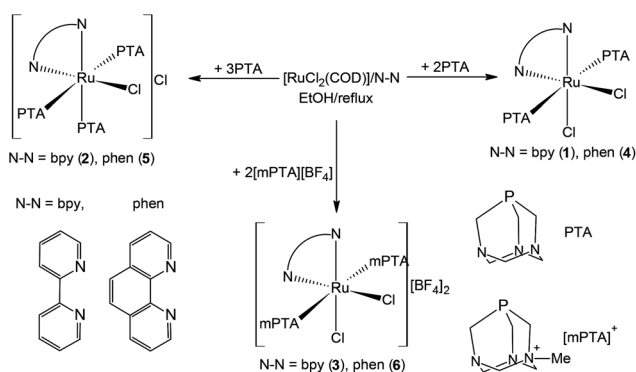
Scheme 1 Synthetic route for compounds **1–6** and their structural formulae.

2.2. X-ray diffraction study

Compounds **1**, **3**, **5** and **6** were obtained in crystalline form and structurally characterized by single-crystal X-Ray diffraction measurements. Crystallographic data for all complexes are presented in Table 1 whereas selected geometrical parameters are listed in Table 2. Fig. 2–5 depict ellipsoid diagrams (drawn at 30% probability level) of compounds **1**, **3**, **5** and **6**. In all the crystal structures the ruthenium center is six-coordinated in a rather distorted octahedral geometry (Fig. 1).

2,2′-Bipyridine (bpy) and 1,10-phenanthroline (phen) always act as bidentate κ²*N*,*N*-ligands. In compounds **1**, **3** and **6** two phosphine ligands bind to Ru(II) in axial positions through phosphorus atoms. In complex **5** three PTA molecules bind to the metal, the first two occupying the axial positions, and the third one, the equatorial position.

The coordination spheres are completed by chloride ligands. Complex **1** (Fig. 2) crystallizes in the monoclinic crystal system, $P2_1/n$ space group. **1** crystallizes as a toluene solvate, with one toluene molecule per two metallic centres. In the equatorial plane one bidentate κ²*N*³¹,*N*³² bpy molecule and two chlorides bind to the Ru center. The two P-donor PTA in the *trans* position complete the coordination sphere. Bond length and angle values suggest a rather distorted octahedral environment. Quadratic elongation and angle variance parameters describing the distortion in coordination polyhedra[37] are 1.010 and 17.62 [deg²] respectively. The bond length average values for Ru–Cl [2.4353(19) Å], Ru–P [2.3126(17) Å] and Ru–N [2.032(5) Å] are consistent with the tabulated typical interatomic distances for organometallic compounds and complexes 2.416(49) Å, 2.307(50) Å and 2.124(49) Å, respectively.[38] Complex **3** (Fig. 3)

Table 2 Selected geometrical parameters for **1**, **3**, **5** and **6**

Compound	Bond distances [Å]		Valence angles [°]	
1	Ru1–P11	2.3056(18)	P11–Ru1–P21	177.86(6)
	Ru1–P21	2.3202(18)	N31–Ru1–Cl1	173.09(16)
	Ru1–Cl1	2.4211(18)	N32–Ru1–Cl2	176.00(16)
	Ru1–Cl2	2.4480(17)	N31–Ru1–N32	79.4(2)
	Ru1–N31	2.035(5)	Cl1–Ru1–Cl2	89.57(6)
	Ru1–N32	2.031(5)		
3	Ru1–P11	2.304(6)	P11–Ru1–P21	173.01(19)
	Ru1–P21	2.313(6)	N31–Ru1–Cl1	174.4(5)
	Ru1–Cl1	2.435(5)	N32–Ru1–Cl2	174.7(5)
	Ru1–Cl2	2.438(6)	N31–Ru1–N32	79.1(5)
	Ru1–N31	2.059(17)	Cl1–Ru1–Cl2	89.78(16)
	Ru1–N32	2.050(16)		
5, cation 1	Ru1–P11	2.345(3)	P11–Ru1–P31	172.15(12)
	Ru1–P21	2.269(3)	N72–Ru1–P21	176.2(3)
	Ru1–P31	2.353(3)	N71–Ru1–Cl1	169.8(2)
	Ru1–Cl1	2.439(3)	P21–Ru1–N71	97.4(2)
	Ru1–N71	2.108(9)	P21–Ru1–Cl1	92.18(12)
	Ru1–N72	2.147(9)	N72–Ru1–Cl1	91.4(3)
			N71–Ru1–N72	79.0(4)
Cation 2	Ru2–P41	2.333(3)	P41–Ru2–P61	172.15(12)
	Ru2–P51	2.279(3)	N82–Ru2–P51	177.1(3)
	Ru2–P61	2.356(3)	N81–Ru2–Cl2	170.2(3)
	Ru2–Cl2	2.437(3)	P51–Ru2–N81	97.9(3)
	Ru2–N81	2.049(10)	P51–Ru2–Cl2	91.93(12)
	Ru2–N82	2.144(9)	N82–Ru2–Cl2	90.9(3)
			N81–Ru2–N82	79.2(4)
6	Ru1–P1	2.3020(13)	P1–Ru1–P1ⁱ	172.15(4)
	Ru1–Cl1	2.4479(9)	N11–Ru1–Cl1ⁱ	173.58(7)
	Ru1–N11	2.065(3)	N11ⁱ–Ru1–Cl1	173.58(7)
			N11ⁱ–Ru1–N11ⁱ	79.77(15)
			Cl1–Ru1–Cl1ⁱ	91.60(5)

Symmetry code: (i) −*x* + 1, *y*, −*z* + 1.5.

Table 1 Crystallographic data for **1**, **3**, **5** and **6**

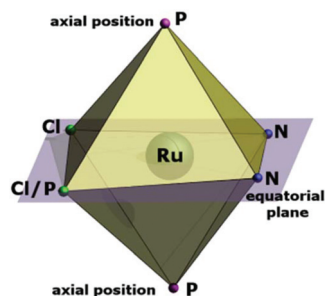|	**1**	**3**	**5**	**6**
Formula	$C_{51}H_{72}Cl_4N_{16}P_4Ru_2$	$C_{24}H_{38}B_2Cl_2F_8N_8P_2Ru$	$C_{30}H_{44}Cl_2N_{11}P_3Ru$	$C_{26}H_{40}B_2Cl_2F_8N_8O_1P_2Ru$
Moiety formula	$2[RuCl_2\{P(CH_2)_6N_3\}_2(C_{10}H_8N_2)]\cdot C_7H_8$	$[RuCl_2\{P(CH_2)_6N_2NCH_3\}_2(C_{10}H_8N_2)](BF_4)_2$	$[RuCl\{P(CH_2)_6N_3\}_3(C_{12}H_8N_2)]Cl$	$([RuCl_2\{P(CH_2)_6N_2NCH_3\}_2(C_{12}H_8N_2)](BF_4)_2)\cdot H_2O$
FW [g mol⁻¹]	1377.06	846.15	823.64	888.17
T [K]	100(2)	250(2)	100(2)	120(2)
Wavelength [Å]	0.71073	0.71073	0.71073	0.71073
Cryst. syst.	Monoclinic	Orthorhombic	Monoclinic	Monoclinic
Space group	$P2_1/n$	$Pna2_1$	$P2_1/n$	$C2/c$
a [Å]	12.908(3)	15.430(4)	24.786(5)	20.995(5)
b [Å]	17.662(4)	9.266(3)	11.296(3)	19.804(5)
c [Å]	13.355(2)	23.561(5)	29.376(6)	8.763(3)
β [°]	109.96(3)°		93.79(3)	110.77(3)
V [Å³]	2861.8(11)	3368.6(16)	8207(3)	3406.7(18)
Z	2	4	8	4
Calcd [g cm⁻³]	1.598	1.668	1.333	1.728
μ [mm⁻¹]	0.879	0.795	0.664	0.793
T_{min}/T_{max}	0.774/0.967	0.961/0.977	0.925/0.961	0.793/0.813
θ range [°]	2.820–24.996	2.706–24.992	2.837–25.000	2.922–24.999
Reflns collected	9238	8933	49 399	9702
Indep reflns (R_{int})	4822 (0.0686)	4568 (0.1143)	14 412 (0.2404)	2990 (0.0497)
GOF on F^2	1.036	0.949	0.999	1.044
Final R_1/wR_2 indices	0.0591/0.1316	0.0674/0.1302	0.0920/0.2609	0.0438/0.1214

Fig. 1 The coordination sphere of the Ru(II) centre in **1**, **3**, **5** and **6**.
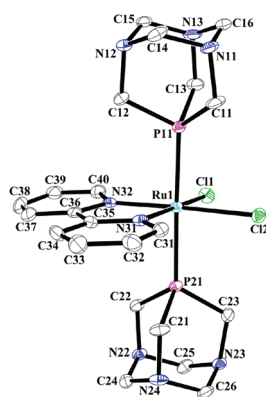

Fig. 2 Ellipsoid diagram (drawn at the 30% probability level) of **1**. Hydrogen atoms and toluene molecules are omitted for clarity.
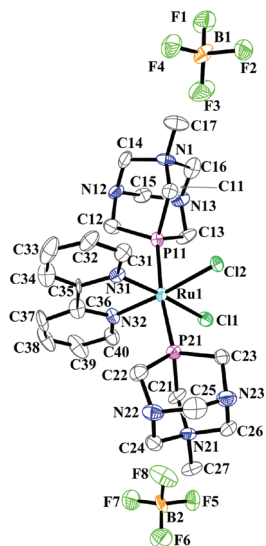

Fig. 3 Ellipsoid diagram (drawn at the 30% probability level) of **3**. Hydrogen atoms are omitted for clarity.

crystallizes in the orthorhombic crystal system, in the achiral non-centrosymmetric space group.[39] The Flack parameter 0.48(9), determined using 554 quotients $[[(I+) - (I-)]/[(I+) + (I-)]]$,[40] suggests that the crystal is an inversion twin consisting of crystalline domains related by a center of symmetry.[41]
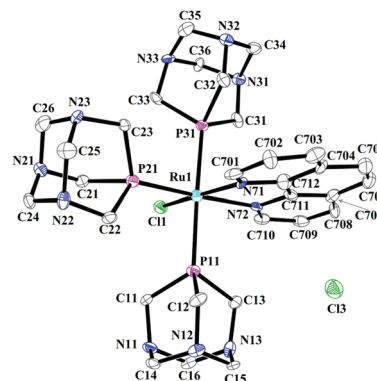

Fig. 4 Ellipsoid diagram (drawn at the 30% probability level) of **5**. Hydrogen atoms are omitted for clarity. Figure contains only one molecule.

The asymmetric unit consists of one cationic Ru(II) complex and two BF_4^- counterions. The Ru coordination sphere is a rather distorted octahedron (values of quadratic elongation and angle variance are 1.011 and 21.96 $[deg^2]$ respectively). The ligand arrangement around the Ru(II) center is similar to that previously described in complex **1**.

One bidentate $\kappa^2 N^{31}, N^{32}$-bpy molecule and two chloride ligands bind to the metal in equatorial positions, with two mPTA molecules coordinating through the phosphorus atom in the axial position. Bond length average values of Ru–Cl [2.4365(18) Å], Ru–P [2.308(6) Å] and Ru–N [2.055(6) Å] are similar to typical literature distances [2.416(49) Å, 2.307(50) Å and 2.124(49) Å respectively].[38] Complex **5** (Fig. 4) crystallizes in the monoclinic crystal system, $P2_1/n$ space group. The asymmetric unit contains two cationic Ru coordination centers and two chlorine counter-ions. The Ru(II) coordination sphere in both cations consists of six donor atoms arranged in a distorted octahedron, with phen binding to the metal ion in a bidentate $\kappa^2 N, N$ fashion. Three PTA molecules coordinate to Ru(II) as κP ligands, two of them in the axial position, the remaining one in the equatorial plane. One Cl bonds to the Ru coordination sphere, the other acting as a counterion.

Distortion parameters are: quadratic elongation 1.010 (for both residues) and angle variance 23.18 $[deg^2]$ and 22.75 $[deg^2]$ respectively for cations 1 (Ru1) and 2 (Ru2). The average values of bond lengths Ru–Cl [2.438 Å], Ru–P [2.323(39) Å] and Ru–N [2.112 (46) Å] are consistent with the typical values for organometallic compounds presented in the literature [2.416(49) Å, 2.307(50) Å and 2.124(49) Å, respectively].[38] The Ru1–P11 and Ru1–P31 (Ru2–P41 and Ru2–P61 in cation 2) axial distances are slightly longer than the equatorial Ru1–P21 (Ru2–P51) bond because the *trans* effect of phosphine ligands is stronger than that of the heterocyclic nitrogen atom. Complex **6** (Fig. 5) crystallizes in the monoclinic crystal system, $C2/c$ space group. **6** exhibits a molecular symmetry C_2, with a 2-fold rotational axis present in the equatorial plane passing through the Ru atom and phen. In the crystal the [RuCl(phen)(PTA)₃]⁺⁺ ion is accompanied by two BF_4^- counterions and one water
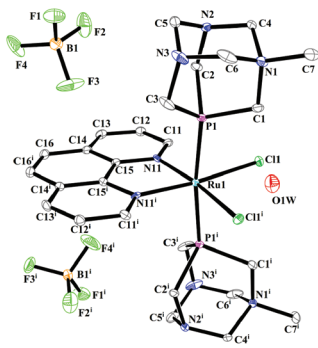
Fig. 5 Ellipsoid diagram (drawn at the 30% probability level) of **6**, symmetry code: (i) $-x + 1$, y, $-z + 1.5$. Hydrogen atoms are omitted for clarity.

molecule. The arrangement of the ligands around the metal ion is analogous to that observed in **1** and **3**.

One phen molecule binds the metal as a bidentate $\kappa^2 N^{11}$, N^{11i}-ligand in the equatorial plane, whereas the two mPTA are coordinate to Ru as κP ligands in the axial position. The distorted octahedral Ru coordination sphere is completed by two chloride ligands (values of quadratic elongation and angle variance are 1.010 and 20.36 [$\deg^2$] respectively). The bond length values Ru–Cl [2.4479(9) Å], Ru–P [2.3020(13) Å] and Ru–N [2.065(3) Å] are in good agreement with the tabulated data [2.416(49) Å, 2.307(50) Å and 2.124(49) Å respectively].[38]

The electronic absorption spectra of complexes **1–6** have been recorded in DMSO in the UV-Vis region of 220–700 nm (Fig. 1S ESI†). The wavelength (λ_{max}) and molar absorption values (ε) of the complexes are reported in Table 1S (ESI†). For all Ru-complexes, the spectra show two major absorption bands, one intense band around at 260–310 nm that could be due to π–π^* electronic transition and one less intense band in the 400–500 nm range that is mainly associated with the n–π^* transition type.[42]

2.3. Cytotoxicity studies

The ability of ruthenium complexes **1–6** used at different doses to affect the viability of MM cells was evaluated by the MTT assay. Our results evidenced that the Ru complexes showed different abilities in reducing cell viability in the MM cell lines. The most effective Ru complex in reducing cell viability was **4** (Table 3) followed by **5**, **2**, and **1**. Low cytotoxic effects were observed for **6** and **3**, which showed a high IC$_{50}$ value compared with that of the other tested compounds. We found that **1–6** were able, with different potencies, to reduce cell viability in the MM cell lines. All data suggest that **4** was the most effective in blocking cell cycles and in inducing necrotic cell death in the MM cell lines. In addition, we evidenced that all the compounds tested were more effective than cisplatin, which was used as a positive control (Table 3).

2.3.1. Ru-complexes in cell cycle and cell death, in MM cell lines. According to the MTT data, we decided to investigate the cytotoxic mechanism of the most active Ru complexes (**1**, **2**, **4**

Table 3 Cytotoxicity (IC$_{50}$, μM) of **1–6** determined at 72 hours post-treatment in U266 and RPMI cell lines. Cell viability was determined by the MTT assay. Data shown are expressed as mean ± SE of three separate experiments

Compound	IC$_{50}$ (U266) [μM]	IC$_{50}$ (RPMI) [μM]
1	197.6 ± 12	160.5 ± 14
2	192.5 ± 14	140.9 ± 11
3	$181 \times 10^3 \pm 15$	$159 \times 10^3 \pm 12$
4	98.4 ± 6	65.8 ± 5
5	120.5 ± 8	82.3 ± 4
6	$119 \times 10^3 \pm 13$	$115.2 \times 10^3 \pm 10$
Cisplatin	632.7 ± 22	265.5 ± 13

and **5**), excluding Ru complexes **3** and **6** from this analysis. The role of Ru complexes **1**, **2**, **4** and **5** in influencing cell cycles was analyzed by PI staining and FACS analysis after 48 h of treatment in both cell lines. As shown in Fig. 6S,† **4** and **5** were more effective in influencing the cell cycle phase than **1** and **2**. In particular, we found that **1**, **2**, **4** and **5**, with different potencies, induced an accumulation in the sub-G0 phase (hypodiploid DNA) and in the G0/G1 phase, suggesting an effect in blocking cell cycles and in inducing cell death, in RPMI cells. In U266, the compounds **4** and **5** were more effective in increasing the percentage of cells in the G0/G1 phase with respect to **1** and **2**, indicating an effect in blocking cell cycles, while no sub-G0 cell accumulation was detected, at 48 hours post-treatment. These data evidenced that RPMI were more sensitive than U266 to Ru complex treatments, since in RPMI an induction of cell death was detected, while in U266 the Ru complexes were able to block cell cycles but did not induce cell death at 48 hours post-treatment. To further investigate the potential role of compounds **1**, **2**, **4** and **5** in inducing cell death, we analyzed the treated cell lines with PI/annexin-V staining, at 72 h post-treatment. The results show that an increase in PI$^+$/Ann-V$^-$ (necrotic cells) was observed in compound **4**-treated cells, while low or no effect was evidenced with the other Ru complexes in both cell lines (Fig. 2S and 3S†). The data indicate that the only Ru complex **4** was effective in inducing necrotic cell death, at 72 h post-treatment, in both cell lines. All data suggest that **4** was the most effective in blocking cell cycles and in inducing necrotic cell death in the MM cell lines.

For the accurate bioavailability and biological activity of potential drugs, a balanced solubility in both water and non-polar compounds such as lipids is also required.[43a] The activity of the ruthenium complexes described here could also be related to the strongly negative log P values of **1–6**, in contrast to the other, described in the literature, with more balanced log P factors.[43a]

3.   Conclusions

In summary we have successfully synthesized six novel ruthenium(II) complexes containing bipyridyl ligands and PTA. These compounds have been structurally and spectroscopically

characterized, and in all cases a distorted octahedron was found, also if neutral, cationic or dicationic species were obtained. The antitumor activity of selected species has been evaluated *in vitro* against U266 and RPMI human myeloma cells; compound **4** was the most effective in blocking cell cycles and in inducing necrotic cell death in MM cell lines.

4. Experimental

4.1. Materials and methods

All synthetic work was performed under an inert atmosphere of dry oxygen-free dinitrogen, using standard Schlenk techniques. Solvents were dried and distilled prior to use. 2,2′-Bipyridine (bpy) and 1,10-phenanthroline (phen) were obtained from Aldrich and used as received, while $[RuCl_2(COD)]_n$,[43b] PTA,[44,45] and *N*-methyl-1,3,5-triaza-7-phosphaadamantane tetrafluoroborate $\{[mPTA](BF_4)\}$[46] were synthesized in accordance with literature methods. Elemental analyses were performed on a Vario EL III apparatus. Positive electrospray mass spectra were obtained with a Bruker MicroOTOF-Q instrument, using a methanol mobile phase. Infrared spectra (4000–400 cm^{-1}) were recorded on a Bruker IFS 1113v instrument in KBr pellets, whereas ^{1}H and ^{31}P{^{1}H} NMR spectra were recorded on a Bruker Avance 500 MHz spectrometer at ambient temperature (~25 °C). ^{1}H chemical shifts (δ) are expressed in ppm relative to Si(Me)$_4$, while δ(^{31}P) are relative to an external 85% aqueous H$_3$PO$_4$ solution. Coupling constants are in Hz; abbreviations: s, singlet; d, doublet; t, triplet; dd, doublet of doublets, m, multiplet; br, broad.

4.2. Syntheses of ruthenium complexes 1–6

[RuCl$_2$(bpy)(PTA)$_2$] (1). A suspension of $[RuCl_2(COD)]_n$ (56 mg, 0.2 mmol) and bpy (32 mg, 0.2 mmol) in ethanol (50 mL) was refluxed for 8 h under an N$_2$ atmosphere. Then PTA was added (64 mg, 0.4 mmol) and refluxing of the reaction mixture continued for 4 h. Slow evaporation of the resulting dark-red solution afforded an orange microcrystalline solid, which was washed with toluene (2 × 5 mL), then diethyl ether (3 × 5 mL), and dried *in vacuo*. Yield: **1**, 45% (58 mg, 0.090 mmol) based on $[RuCl_2(COD)]_n$. **1** is soluble in H$_2$O ($S_{25\,°C} \approx 12$ mg mL^{-1}), DMSO and CHCl$_3$, MeOH and EtOH, and insoluble in diethyl ether, C$_6$H$_6$ and alkanes. C$_{22}$H$_{32}$Cl$_2$N$_8$P$_2$Ru (FW 642.5): calcd C 41.13, H 5.02, N 17.44; found C 41.21, H 4.98, N 17.40. IR (KBr) 3422 br m, 2919m, 1636m, 1469w, 1447m, 1420m, 1410m, 1361w, 1282s, 1243vs, 1097s, 1044m, 1016vs, 975vs, 948vs, 899m, 887m, 811s, 746s, 579s, 565s, 462m cm^{-1}. ^{1}H NMR (500.13 MHz, DMSO-d$_6$): δ 9.49 (d, 2H, $^{6,6'}$H, $^3J_{6-5} = 5.7$ Hz, bpy), 8.41 (d, 2H, $^{3,3'}$H, $^3J_{3-4} = 7.6$ Hz, bpy), 8.13 (ddd, 2H, $^{4,4'}$H, $^3J_{4-5} = ^3J_{4-3} = 7.6$ Hz, $^4J_{4-6} = 1.5$ Hz, bpy), 7.66 (ddd, 2H, $^{5,5'}$H, $^3J_{5-6} = ^3J_{5-4} = 5.7$ Hz, $^4J_{5-3} = 1.5$ Hz, bpy), 4.26 and 4.11 (2d, 12H, $J_{AB} = 12.0$ Hz, NCH^{A}H^{B}N, PTA), 3.52 (s, 12H, PCH$_2$N, PTA). ^{13}C{^{1}H} NMR (125.76 MHz, DMSO-d$_6$): 155.1 (s, $^{2,2'}$C, bpy), 149.0 (s, $^{6,6'}$C, bpy), 134.3 (s, $^{4,4'}$C, bpy), 125.0 (s, $^{3,3'}$C, bpy), 123.0 (s, $^{5,5'}$C,

bpy), 72.8 (d, $J_{CP} = 7.4$ Hz, NCH$_2$N, PTA,), 51.9 (d, $J_{CP} = 13.0$ Hz, PCH$_2$N, PTA). ^{31}P{^{1}H} NMR (202.46 MHz, DMSO-d$_6$): δ −53.3 (s). ESI-MS$^+$ CH$_3$OH (*m/z* [relative intensity, %]): 450[20] [RuCl(bpy)(PTA)]$^+$, 508[85] [RuCl$_2$(bpy)(PTA)Na]$^+$, 607[70] [RuCl(bpy)(PTA)$_2$]$^+$, 643[90] [RuCl$_2$(bpy)(PTA)$_2$H]$^+$, 667[100] [RuCl$_2$(bpy)(PTA)$_2$Na]$^+$.

[RuCl(bpy)(PTA)$_3$]Cl (2). A suspension of $[RuCl_2(COD)]_n$ (56 mg, 0.2 mmol) and bpy (32 mg, 0.2 mmol) in ethanol (50 mL) was refluxed for 1 h under an N$_2$ atmosphere. Then PTA was added (96 mg, 0.6 mmol) and refluxing of the reaction mixture continued for 2 h. Slow evaporation of the resulting dark-red solution afforded a dark-orange microcrystalline solid, which was washed with toluene (2 × 10 mL), then diethyl ether (4 × 5 mL), and then dried *in vacuo*. Yield: **2**, 70% (112 mg, 0.140 mmol) based on $[RuCl_2(COD)]_n$. **2** is soluble in H$_2$O ($S_{25\,°C} \approx 13$ mg mL^{-1}), DMSO and CHCl$_3$, MeOH and EtOH, and insoluble in diethyl ether, C$_6$H$_6$ and alkanes. C$_{28}$H$_{44}$Cl$_2$N$_{11}$P$_3$Ru (FW 799.6): calcd C 42.06, H 5.55, N 19.27; found C 41.99, H 5.62, N 19.22. IR (KBr): 3421 br, 2919m, 1635m, 1446m, 1420m, 1049m, 1362w, 1280s, 1242s, 1096m, 1043w, 1031w, 970s, 934s, 898m, 810s, 746s, 579s, 484w, 462w. ^{1}H NMR (500.13 MHz, DMSO-d$_6$): δ 9.44 (br, d, 2H, ^{6}H, $^3J_{6-5} = 5.3$ Hz, bpy), 8.73 (d, 2H, ^{3}H, $^3J_{3-4} = 8.4$ Hz, bpy), 8.61 (d, 2H, $^{3'}$H, $^3J_{3'-4'} = 8.4$ Hz, bpy), 8.51 (br, d, 2H, $^{6'}$H, $^3J_{6-5'} = 5.7$ Hz, bpy), 8.35 (dd, 2H, ^{4}H, $^3J_{4-5} = ^3J_{4-3} = 7.6$ Hz, bpy), 8.11 (dd, 2H, $^{4'}$H, $^3J_{4'-5'} = ^3J_{4'-3'} = 7.4$ Hz, bpy), 7.87 (dd, 2H, ^{5}H, $^3J_{5-6} = ^3J_{5-4} = 6.5$ Hz, bpy), 7.50 (dd, 2H, $^{5'}$H, $^3J_{5'-6'} = ^3J_{5'-4'} = 6.7$ Hz, bpy), 4.60–3.50 (m, 36H, NCH^{A}H^{B}N and PCH$_2$N, PTA). ^{13}C{^{1}H} NMR (125.76 MHz, DMSO-d$_6$): 156.9 (s, $^{2,2'}$C, bpy), 151.8 (s, $^{6,6'}$C, bpy), 135.8 (s, $^{4,4'}$C, bpy), 124.8 (s, $^{3,3'}$C, bpy), 122.9 (s, $^{5,5'}$C, bpy), 75.0 (br s, NCH$_2$N, PTA), 57.0 (br s, PCH$_2$N, PTA). ^{31}P{^{1}H} NMR (202.46 MHz, DMSO-d$_6$): δ −38.2 (t), −57.4 (d), $^2J_{P-P} = 34.8$ Hz. ESI-MS$^+$ CH$_3$OH (*m/z* [relative intensity, %]): 450[15] [RuCl(bpy)(PTA)]$^+$, 607.1[100] [RuCl(bpy)(PTA)$_2$]$^+$, 764.2[80] [RuCl(bpy)(PTA)$_3$]$^+$.

[RuCl$_2$(bpy)(mPTA)$_2$](BF$_4$)$_2$ (3). A suspension of $[RuCl_2(COD)]_n$ (56 mg, 0.2 mmol) and bpy (32 mg, 0.2 mmol) in ethanol (50 mL) was refluxed for 6 h under an N$_2$ atmosphere. Then $\{[mPTA](BF_4)\}$ was added (103.6 mg, 0.4 mmol) and refluxing of the reaction mixture continued for 3 h. Slow evaporation of the resulting dark-red solution afforded an orange microcrystalline solid, which was washed with toluene (2 × 10 mL), then diethyl ether (4 × 5 mL), and dried *in vacuo*. Yield: **3**, 80% (135 mg, 0.160 mmol) based on $[RuCl_2(COD)]_n$. **3** is soluble in H$_2$O ($S_{25\,°C} \approx 14$ mg mL^{-1}), DMSO and CHCl$_3$, MeOH and EtOH, and insoluble in diethyl ether, C$_6$H$_6$ and alkanes. C$_{22}$H$_{42}$B$_2$Cl$_2$F$_8$N$_6$P$_2$Ru (FW 846.1): calcd C 34.07, H 4.53, N 13.24; found C 33.98, H 4.50, N 12.91. IR (KBr): 3435 br m, 3078w, 2973w, 2923w, 1632w, 1606m, 1467vs, 1446s, 1417s, 1309vs, 1283m, 1270m, 1249w, 1123m, 1096s, 1065 br s, 1031s, 985m, 925s, 897vs, 812s, 768s, 747vs, 567m, 553m, 521m, 463m, 442m, 387w. ^{1}H NMR (500.13 MHz, DMSO-d$_6$): δ 9.30 (d, 2H, $^{6,6'}$H, $^3J_{6-5} = 5.0$ Hz, bpy), 8.55 (d, 2H, $^{3,3'}$H, $^3J_{3-4} = 8.0$ Hz, bpy), 8.08 (ddd, 2H, $^{4,4'}$H, $^3J_{4-5} = ^3J_{4-3} = 8.0$ Hz, $^4J_{4-6} = 1.5$ Hz, bpy), 7.58 (ddd, 2H, $^{5,5'}$H, $^3J_{5-6} = ^3J_{5-4} = 5.0$ Hz, $^4J_{5-3} = 1.5$ Hz, bpy), 4.89 and 4.71 (2d, 8H, $J_{AB} = 11$ Hz,

NCH^{A}H^{B}N$^+$, mPTA), 4.33 and 4.13 (2d, 4H, J_{AB} = 13 Hz, NCH^{A}H^{B}N, mPTA), 4.19 (s, 4 H, PCH$_2$N$^+$, mPTA), 3.51 and 3.47 (2d, 8H, J_{AB} = 15.0 Hz, PCH^{A}H^{B}N, mPTA), 2.62 (s, 6H, N$^+$CH$_3$, mPTA). ^{13}C{^{1}H} NMR (125.76 MHz, DMSO-d_6): 158.9 (s, $^{2,2'}$C, bpy), 152.1 (s, $^{6,6'}$C, bpy), 136.6 (s, $^{4,4'}$C, bpy), 125.5 (s, $^{3,3'}$C, bpy), 123.7 (s, $^{5,5'}$C, bpy), 79.5 (s, NCH$_2$N$^+$, PTA-Me), 68.5 (s, NCH$_2$N, PTA-Me), 52.2, (br s, PCH$_2$N$^+$, PTA-Me), 48.4 (s, N$^+$CH$_3$, PTA-Me), 43.4 (br s, PCH$_2$N, PTA-Me). ^{31}P{^{1}H} NMR (202.46 MHz, DMSO-d$_6$): δ −31.4 (s). ESI-MS$^+$ CH$_3$OH (m/z [relative intensity, %]): 463[100] [RuCl$_2$(bpy)(BF$_4$)Na$_2$$^+$]$^+$, 510[60%] [RuCl$_2$(bpy)(mPTA)]$^+$, 759[30] [RuCl(BF$_4$)$_2$(bpy)(mPTA)$_2$]$^+$.

[RuCl$_2$(phen)(PTA)$_2$] (4). This compound was isolated as a dark-red solid by following the procedure described for **1** using phen (36 mg 0.2 mmol) instead of bpy. Yield: **4**, 50% (67 mg, 0.101 mmol) based on [RuCl$_2$(COD)]$_n$. **4** is soluble in H$_2$O ($S_{25\,°C}$ ≈ 13 mg mL^{-1}), DMSO and CHCl$_3$, MeOH and EtOH, and insoluble in diethyl ether, C$_6$H$_6$ and alkanes. C$_{24}$H$_{32}$Cl$_2$N$_8$P$_2$Ru (FW 666.5): calcd C 43.25, H 4.84, N 16.81; found: C 43.20, H 4.90, N 16.86. IR (KBr) 3413 br m, 2918m, 1772w, 1636m, 1559vw, 1469vw, 1446m, 1420m, 1409m, 1359vw, 1281s, 1243s, 1097s, 1044m, 1016vs, 974vs, 947vs, 899m, 887m, 811m, 746m, 579s, 565s, 462s. ^{1}H NMR (500.13 MHz, DMSO-d$_6$): δ 9.69 (dd, 2H, ^{2,9}H, $^3J_{2-3}$ = $^3J_{9-8}$ = 5.3 Hz, $^4J_{2-4}$ = $^4J_{9-7}$ = 1.0 Hz, phen), 8.56 (dd, ^{4,7}H, 2H, $^3J_{4-3}$ = $^3J_{7-8}$ = 8.0 Hz, $^4J_{4-2}$ = $^4J_{7-9}$ = 1.0 Hz, phen), 8.17 (s, 2H, ^{5,6}H, phen), 8.06 (dd, 2H, ^{3,8}H, $^3J_{3-4}$ = $^3J_{8-7}$ = 8.0 Hz, $^3J_{3-2}$ = $^3J_{8-9}$ = 5.3 Hz, phen), 4.18 and 4.01 (2d, 12H, J_{AB} = 13.0 Hz, NCH^{A}H^{B}N, PTA), 3.40 (s, 12H, PCH$_2$N, PTA). ^{13}C{^{1}H} NMR (125.76 MHz, DMSO-d$_6$): 155.0 (s, ^{2,11}C, phen), 150.2 (s, ^{1,12}C, phen), 132.8 (s, ^{4,9}C, phen), 130.0 (s, ^{5,8}C, phen), 123.1 (s, ^{6,7}C, phen), 121.8 (s, ^{3,10}C, phen), 71.0 (br s, NCH$_2$N, PTA), 55.0 (br s, PCH$_2$N, PTA). ^{31}P{^{1}H} NMR (202.46 MHz, DMSO-d$_6$): δ −53.7 (s). ESI-MS$^+$ CH$_3$OH (m/z [relative intensity, %]): 532[50] [RuCl$_2$(phen)Na]$^+$, 631[20] [RuCl(phen)(PTA)$_2$]$^+$, 691[100] [RuCl$_2$(phen)(PTA)$_2$Na]$^+$.

[RuCl(phen)(PTA)$_3$]Cl (5). This compound was isolated as a dark-red solid by following the procedure described for **2** using phen (36 mg, 0.2 mmol) instead of bpy. Yield: **5**, 65% (107 mg, 0.130 mmol) based on [RuCl$_2$(COD)]$_n$. **5** is soluble in H$_2$O ($S_{25\,°C}$ ≈ 12 mg mL^{-1}), DMSO and CHCl$_3$, MeOH and EtOH, and insoluble in diethyl ether, C$_6$H$_6$ and alkanes. C$_{30}$H$_{44}$Cl$_2$N$_{11}$P$_3$Ru (FW 823.6): calcd C 43.75, H 5.38, N 18.71 found: C 43.79, H 5.33, N 18.80. IR (KBr): 3401 br m, 3048w, 2921m, 1969vw, 1628vw, 1588vw, 1560vw, 1505m, 1496m, 1446m, 1420s, 1339vw, 1284m, 1243s, 1166vw, 1139w, 1097m, 1043m, 1016vs, 973vs, 947vs, 894m, 847s, 810s, 736m, 724m, 705w, 695w, 669vw, 644vw, 620vw, 581s, 567m, 522vw, 483vw, 465m. ^{1}H NMR (500.13 MHz, DMSO-d$_6$): δ 9.72 (d, br, 1H, ^{2}H, $^3J_{2-3}$ = 5.0 Hz, phen), 8.99 (d, 1H, ^{4}H, $^3J_{3-4}$ = 5.0 Hz, phen), 8.97 (d, 1H, ^{9}H, $^3J_{8-9}$ = 5.0 Hz, phen), 8.75 (d, 1H, ^{7}H, $^3J_{7-8}$ = 5.0 Hz, phen), 8.37 and 8.32 (2d, ^{5,6}H, 2H, J_{AB} = 9.0 Hz), 8.23 (dd, 1H, ^{3}H, $^3J_{2-3}$ = 5.0 Hz, $^3J_{3-4}$ = 8.0 Hz, phen), 7.83 (dd, 1H, ^{8}H, $^3J_{7-8}$ = 8.0 Hz, $^3J_{8-9}$ = 5.0 Hz, phen), 4.78 and 4.55 (2d, 6H, J_{AB} = 13.0 Hz, NCH^{A}H^{B}N, PTA), 4.39 (s, 6H, PCH$_2$N, PTA), 4.16 and 4.06 (2d, 12H, J_{AB} = 12.8 Hz, NCH^{A}H^{B}N, PTA), 3.31 (s, 12H, PCH$_2$N, PTA). ^{13}C{^{1}H} NMR (125.76 MHz, DMSO-d$_6$): 153.1

(s, ^{2,11}C, phen), 149.9 (s, ^{1,12}C, phen), 135.5 (s, ^{4,9}C, phen), 129.0 (s, ^{5,8}C, phen), 123.5 (s, ^{6,7}C, phen), 122.4 (s, ^{3,10}C, phen), 73.0 (d, J_{CP} = 7.5 Hz, NCH$_2$N, PTA), 52.8 (d, J_{CP} = 13.0 Hz, PCH$_2$N, PTA). ^{31}P{^{1}H} NMR (202.46 MHz, DMSO-d$_6$): δ −38.3 (t), −58.3 (d), $^2J_{P-P}$ = 34.4 Hz. ESI-MS$^+$ CH$_3$OH (m/z [relative intensity, %]): 631.1[100] [RuCl(bpy)(PTA)$_2$]$^+$, 788.2[30] [RuCl(bpy)(PTA)$_3$]$^+$.

[RuCl$_2$(phen)(mPTA)$_2$](BF$_4$)$_2$ (6). This compound was isolated as a dark-red solid by following the procedure described for **3** using phen (36 mg, 0.2 mmol) instead of bpy. Yield: **6**, 81% (141 mg, 0.162 mmol) based on [RuCl$_2$(COD)]$_n$. **6** is soluble in H$_2$O ($S_{25\,°C}$ ≈ 11 mg mL^{-1}), DMSO and CHCl$_3$, MeOH and EtOH, and insoluble in diethyl ether, C$_6$H$_6$ and alkanes. C$_{26}$H$_{38}$B$_2$Cl$_2$F$_8$N$_8$P$_2$Ru (FW 870.2): calcd C 35.89, H 4.40, N 12.88 found: C 36.0, H 4.50, N 12.92. IR (KBr): 3435 br m, 3023w, 2961w, 1634w, 1573w, 1467m, 1427m, 1387w, 1345w, 1303s, 1286m, 1253m, 1202m, 1119m, 1077 br m, 1035m, 986m, 325s, 900vs, 847s, 807vs, 746vs, 722m, 696w, 645w, 568m, 551m, 522m, 463m, 443m, 388m. ^{1}H NMR (500.13 MHz, DMSO-d$_6$): δ 9.51 (dd, 2H, ^{2,9}H, $^3J_{2-3}$ = $^3J_{9-8}$ = 5.7 Hz, $^4J_{2-4}$ = $^4J_{9-7}$ = 1.1 Hz, phen), 8.72 (dd, ^{4,7}H, 2H, $^3J_{4-3}$ = $^3J_{7-8}$ = 8.0 Hz, $^4J_{4-2}$ = $^4J_{7-9}$ = 1.1 Hz, phen), 8.26 (s, 2H, ^{5,6}H, phen), 7.94 (dd, 2H, ^{3,8}H, $^3J_{3-4}$ = $^3J_{8-7}$ = 8.0 Hz, $^3J_{3-2}$ = $^3J_{8-9}$ = 5.7 Hz, phen), 4.81 and 4.68 (2d, 8H, J_{AB} = 11 Hz, NCH^{A}H^{B}N$^+$, mPTA), 4.21 and 4.05 (2d, 4H, J_{AB} = 14 Hz, NCH^{A}H^{B}N, mPTA), 4.13 (s, 4 H, PCH$_2$N$^+$, mPTA), 3.36 (s, 8H, PCH$_2$N, mPTA), 2.57 (s, 6H, N$^+$CH$_3$, mPTA). ^{13}C{^{1}H} NMR (125.76 MHz, DMSO-d_6): 152.8 (s, ^{2,11}C, phen), 149.5 (s, ^{1,12}C, phen), 134.8 (s, ^{4,9}C, phen), 130.1 (s, ^{5,8}C, phen), 127.5 (s, ^{6,7}C, phen), 124.6 (s, ^{3,10}C, phen), 79.4 (s, NCH$_2$N$^+$, PTA-Me), 68.1 (s, NCH$_2$N, PTA-Me), 52.1 (br s, PCH$_2$N$^+$, PTA-Me), 48.3 (s, N$^+$CH$_3$, PTA-Me), 43.2 (br s, PCH$_2$N, PTA-Me). ^{31}P{^{1}H} NMR (202.46 MHz, DMSO-d$_6$): δ −31.8 (s). ESI-MS$^+$ CH$_3$OH (m/z [relative intensity, %]): 528[70] [RuCl$_2$(phen)(mPTA)]$^+$, 784[15] [RuCl$_2$(BF$_4$)(phen)(mPTA)$_2$]$^+$.

4.3. X-ray crystal structure determination

X-ray-quality crystals of **1**, **3**, **5** and **6** were grown by slow evaporation of a sample of reaction solution with the addition of n-octane in conical tubes in air for several days. Single crystal X-Ray diffraction data were collected using a Kuma KM4CCD four-circle diffractometer with Mo Kα radiation and a CCD camera (Sapphire), for compounds **5** and **6** and an Xcalibur four-circle diffractometer with Mo Kα radiation and a CCD camera (Ruby), for compounds **1** and **3**. Measurements for **1** and **5** were carried out at 100 K, for compound **6** at 120 K and for compound **3** at 250 K using an Oxford Cryosystem adapter.[47] Programmes used for data collection and data reduction: CrysAlis CCD, Oxford Diffraction Ltd; CrysAlis RED, Oxford Diffraction Ltd; and CrysAlisPro, Agilent Technologies.[48] Structures were solved by direct methods using the SHELXS program and then refined by a full-matrix least squares method using the SHELXL-2015/1 program with anisotropic thermal parameters for nonhydrogen atoms.[49,50] Molecular graphics were prepared using the XP[51] and Diamond[52] programs. Data for publication were prepared

using the programs SHELXL-2015/1 [49,50] and PLATON.[53] The crystal structure of **5** contains large solvent accessible voids occupied by disordered solvent molecules. These molecules were removed from the final refinement and PLATON SQUEEZE was used to correct the data.[54]

4.4. Stability tests of the complexes with oxygen and water

The ruthenium complexes **1–6** were air stable at least for one year in the solid state and for months in DMSO-d_6 with addition of deuterated water. In a general procedure, the complex was introduced into a NMR tube and dissolved in 0.5 mL of DMSO-d_6 and 0.2 mL of D_2O under an air atmosphere. $^{31}P\{^1H\}$ NMR showed that no evident changes were produced in one month at room temperature. The effect of pH on the stability of **1–6** was also monitored by NMR spectroscopy, using diluted DCl and NaOD solutions. No dramatic changes were observed in the pH range ±2 (apart from a slight shift of the resonances).

4.5. Octanol–water partition coefficient determination

The log P values corresponding to the octanol–water partition coefficient were adjusted to the solubility properties of the compounds.[55] Complexes were dissolved in water previously saturated with octanol at a concentration of 10^{-4} M. Into a 50 mL flask at 24 °C with a magnetic stir bar was introduced initially 10 mL of octanol previously saturated with water and then 10 mL of the complex solutions in water. The two-phase mixture was stirred vigorously for 10 min and samples, which were measured by UV-Vis spectroscopy, were taken from the separated phases. The values of log P have been found to be −2.19, −2.20, −2.80, −2.17, −2.20, and −2.75 for **1–6**, respectively.

4.6. Cell culture

Cells. RPMI8226 (RPMI) and U266 MM cell lines (purchased from ATCC, LGC Standards, Milan, IT). Cell authentication was performed by IST (Genova, Italy). Cell lines were cultured in RPMI medium (Lonza, Milan, IT) supplemented with 10% fetal bovine serum (FBS), 2 mM L-glutamine, 100 IU ml^{-1} penicillin, 100 μg streptomycin and 1 mM sodium pyruvate. The cell lines were maintained at 37 °C with 5% CO_2 and 95% humidity.

Sample preparation. Ru(II) complexes **1–6** were dissolved at 50 mM concentration in DMSO, aliquoted and stored at 4 °C until use.

MTT assay. 3×10^4 cells per ml were seeded in 96-well plates, in a final volume of 100 μL. After 1 day of incubation, Ru(II) complexes at different doses (from 100 nM to 1 M) or the relative vehicle were added and cell viability was evaluated up to 72 h. Four replicate wells were used for each treatment. At the indicated time point, cell viability was assessed by adding 0.8 mg ml^{-1} of MTT (Sigma-Aldrich) to the media. After 3 h, the plates were centrifuged, the supernatant was discharged, and the pellet was solubilized in 100 μl per well of DMSO. The absorbance of the samples against a background control (medium alone) was measured at 570 nm using

an ELISA reader microliter plate (BioTek Instruments, Winooski, VT).

Statistical analysis. The data presented represent the mean and standard deviation (SD) of at least 3 independent experiments. Statistical significance was determined by Student's t-test; *, #, §$p < 0.01$. The statistical analysis of IC$_{50}$ levels was performed using Prism 5.0a (Graph Pad).

Cell cycle analysis. U266 and RPMI cell lines (4×10^4 cells per ml) were incubated with the appropriate Ru complexes for up to 48 hours. Cells were fixed for 1 h by adding ice-cold 70% ethanol and then washed with staining buffer (PBS, 2% FBS and 0.01% NaN$_3$). The cells were treated with 100 μg ml^{-1} ribonuclease A solution (Sigma Aldrich), incubated for 30 min at 37 °C, stained for 30 min at room temperature with 20 μg ml^{-1} propidium iodide (PI) (Sigma Aldrich) and analysed on a FACScan flow cytometer using CellQuest software.

Cell death assays. After treatment with the appropriate Ru complexes for up to 72 h, 4×10^4 U266 and RPMI cells per ml were incubated in a binding buffer containing 20 μg ml^{-1} PI for 10 min at room temperature. The cells were stained with 5 μl of Annexin V FITC (Vinci Biochem, Vinci, Italy) for 10 min at room temperature, washed once with binding buffer (10 mM N-(2-hydroxyethyl)piperazine-N^0-2-ethanesulfonic acid [HEPES]/sodium hydroxide, pH 7.4 and 140 mM NaCl, 2.5 mM CaCl$_2$) and analysed on a FACScan flow cytometer using CellQuest software. Four replicates were used for each treatment.

Conflict of interest

The manuscript was written through contributions of all authors. All authors have given approval to the final version of the manuscript. The authors declare no competing financial interest.

Acknowledgements

References

1 N. J. Wheate, S. Walker, G. E. Craig and R. Oun, *Dalton Trans.*, 2010, **39**, 8113–8127.
2 J. J. Wilson and S. J. Lippard, *Chem. Rev.*, 2013, **114**, 4470–4495.
3 M. Ober and S. J. Lippard, *J. Am. Chem. Soc.*, 2008, **130**, 2851–2861.
4 E. Alessio, *Eur. J. Inorg. Chem.*, 2017, 1549–1560.
5 S. Betanzos-Lara, L. Salassa, A. Habtemariam, O. Novakova, A. M. Pizarro, G. J. Clarkson, B. Liskova, V. Brabec and P. J. Sadler, *Organometallics*, 2012, **31**, 3466–3479.

6 S. Betanzos-Lara, O. Novakova, R. J. Deeth, A. M. Pizarro, G. J. Clarkson, B. Liskova, V. Brabec, P. J. Sadler and A. Habtemariam, *J. Biol. Inorg. Chem.*, 2012, **17**, 1033–1051.

7 M. V. Babak, D. Plazuk, S. M. Meier, H. J. Arabshahi, J. Reynisson, B. Rychlik, A. Błauz, K. Szulc, M. Hanif, S. Strobl, A. Roller, B. K. Keppler and C. G. Hartinger, *Chem. – Eur. J.*, 2015, **21**, 5110–5117.

8 S. M. Meier, M. S. Novak, W. Kandioller, M. A. Jakupec, A. Roller, B. K. Keppler and C. G. Hartinger, *Dalton Trans.*, 2014, **43**, 9851–9855.

9 B. S. Murray, M. V. Babak, C. G. Hartinger and P. J. Dyson, *Coord. Chem. Rev.*, 2016, **306**, 86–114.

10 G. S. Smith and B. Therrien, *Dalton Trans.*, 2011, **40**, 10793–10800.

11 S. K. Singh and D. S. Pandey, *RSC Adv.*, 2014, **4**, 1819–1840.

12 M. U. Raja, B. Therrien and G. Süss-Fink, *Inorg. Chem. Commun.*, 2013, **29**, 194–196.

13 G. Süss-Fink, *Dalton Trans.*, 2010, **39**, 1673–1688.

14 C. S. Chow and F. M. Bogdan, *Chem. Rev.*, 1997, **97**, 1489–1514.

15 C. Kaes, A. Katz and M. W. Hosseini, *Chem. Rev.*, 2000, **100**, 3553–3590.

16 G. Chelucci and R. P. Thummel, *Chem. Rev.*, 2002, **102**, 3129–3170.

17 M. R. Gill and J. A. Thomas, *Chem. Soc. Rev.*, 2012, **41**, 3179–3192.

18 J. Bravo, S. Bolaño, L. Gonsalvi and M. Peruzzini, *Coord. Chem. Rev.*, 2010, **254**, 555–607.

19 B. S. Murray, M. V. Babak, C. G. Hartinger and P. J. Dyson, *Coord. Chem. Rev.*, 2016, **306**, 86–114.

20 W.-C. Lee, J. M. Sears, R. A. Enow, K. Eads, D. A. Krogstad and B. J. Frost, *Inorg. Chem.*, 2013, **52**, 1737–1746.

21 A. García-Fernández, J. Díez, M. P. Gamasa and E. Lastra, *Eur. J. Inorg. Chem.*, 2014, **2014**, 917–924.

22 J. Huang, J. Chen, H. Gao and L. Chen, *Inorg. Chem.*, 2014, **53**, 9570–9580.

23 F. Scalambra, M. Serrano-Ruiz, S. Nahim-Granados and A. Romerosa, *Eur. J. Inorg. Chem.*, 2016, 1528–1540.

24 M. S. Raab, K. Podar, I. Breitkreutz, P. G. Richardson and K. C. Anderson, *Lancet*, 2009, **374**, 324–339.

25 S. V. Rajkumar, *Am. J. Hematol.*, 2016, **91**, 90–100.

26 Y. K. Yan, M. Melchart, A. Habtemariam and P. J. Sadler, *Chem. Commun.*, 2005, 4764–4776.

27 A. Martínez, C. S. Rajapakse, R. A. Sánchez-Delgado, A. Varela-Ramirez, C. Lema and R. J. Aguilera, *J. Inorg. Biochem.*, 2010, **104**, 967–977.

28 R. Pettinari, F. Marchetti, A. Petrini, C. Pettinari, G. Lupidi, B. Fernández, A. R. Diéguez, G. Santoni and M. Nabissi, *Inorg. Chim. Acta*, 2017, **454**, 139–148.

29 M. B. Morelli, M. Offidani, F. Alesiani, G. Discepoli, S. Liberati, A. Olivieri, M. Santoni, G. Santoni, P. Leoni and M. Nabissi, *Int. J. Cancer*, 2014, **134**, 2534–2546.

30 A. D. Phillips, L. Gonsalvi, A. Romerosa, F. Vizza and M. Peruzzini, *Coord. Chem. Rev.*, 2004, **248**, 955–993.

31 A. Lis, M. G. da Silva and A. Kirillov, *Cryst. Growth Des.*, 2010, **10**, 5245.

32 A. M. Kirillov, S. W. Wieczorek, F. C. G. Guedes da Silva, J. Sokolnicki, P. Smoleński and A. J. Pombeiro, *CrystEngComm*, 2011, **13**, 6329–6333.

33 P. Smolenski, F. P. Pruchnik, Z. Ciunik and T. Lis, *Inorg. Chem.*, 2003, **42**, 3318–3322.

34 P. Smoleński, C. Pettinari, F. Marchetti, M. F. C. Guedes da Silva, G. Lupidi, G. V. Badillo Patzmay, D. Petrelli, L. A. Vitali and A. J. L. Pombeiro, *Inorg. Chem.*, 2015, **54**, 434–440.

35 B. J. Coe and S. J. Glenwright, *Coord. Chem. Rev.*, 2000, **203**, 5–80.

36 K. Nakamoto, *Infrared and Raman Spectra of Inorganic and Coordination Compounds: Part B: Applications in Coordination, Organometallic, and Bioinorganic Chemistry*, John Wiley & Sons, Inc., 2008.

37 K. Robinson, G. Gibbs and P. Ribbe, *Science*, 1971, **172**, 567–570.

38 F. Allen, D. Watson, L. Brammer, A. Orpen and R. Taylor, in *International Tables for Crystallography Volume C: Mathematical, physical and chemical tables*, Springer, 2006, pp. 790–811.

39 A. Glazer and K. Stadnicka, *Acta Crystallogr., Sect. A: Fundam. Crystallogr.*, 1989, **45**, 234–238.

40 S. Parsons, H. D. Flack and T. Wagner, *Acta Crystallogr., Sect. B: Struct. Sci., Cryst. Eng. Mater.*, 2013, **69**, 249–259.

41 H. D. Flack and G. Bernardinelli, *Acta Crystallogr., Sect. A: Fundam. Crystallogr.*, 1999, **55**, 908–915.

42 A. Lever, *Inorganic electronic spectroscopy*, 1984, vol. 2, pp. 376–611.

43 (*a*) E. García-Moreno, S. Gascón, M. J. Rodriguez-Yoldi, E. Cerrada and M. Laguna, *Organometallics*, 2013, **32**, 3710–3720; (*b*) S. Komiya, *Synthesis of Organometallic Compounds: A practical Guide*, John Wiley and Sons, 1997.

44 D. Daigle, A. Pepperman and S. L. Vail, *J. Heterocycl. Chem.*, 1974, **11**, 407–408.

45 D. J. Daigle, T. J. Decuir, J. B. Robertson and D. J. Darensbourg, *Inorg. Synth.*, 1998, **32**, 40–45.

46 P. Smoleński, A. M. Kirillov, M. F. C. Guedes da Silva and A. J. Pombeiro, *Acta Crystallogr., Sect. E: Struct. Rep. Online*, 2008, **64**, o556–o556.

47 J. t. Cosier and A. Glazer, *J. Appl. Crystallogr.*, 1986, **19**, 105–107.

48 *P. CrysAlis*, Agilent Technologies Ltd, Yarnton, England, 2014.

49 G. M. Sheldrick, *Acta Crystallogr., Sect. A: Found. Crystallogr.*, 2008, **64**, 112–122.

50 G. M. Sheldrick, *Acta Crystallogr., Sect. C: Cryst. Struct. Commun.*, 2015, **71**, 3–8.

51 *X. I. M. GRAPHICS*, Bruker Analytical X-ray System, 1998.

52 K. Brandenburg and M. Berndt, *J. Appl. Crystallogr.*, 1999, **32**, 1028.

53 A. Spek, *J. Appl. Crystallogr.*, 2003, **36**, 7–13.

54 A. L. Spek, *Crystallogr., Sect. C: Cryst. Struct. Commun.*, 2015, **71**, 9–18.

55 J. Sangster, *J. Phys. Chem. Ref. Data*, 1989, 1111–1227.